Photodegradation of Avermectin B_{1a} Thin Films on Glass

Louis S. Crouch,*,† William F. Feely,† Byron H. Arison,‡ William J. A. VandenHeuvel,‡ Lawrence F. Colwell,§ Ralph A. Stearns,‡ Walter F. Kline,†,∥ and Peter G. Wislocki†

Department of Animal and Exploratory Drug Metabolism, Pesticide Metabolism and Environmental Safety Group, Merck Sharp & Dohme Research Laboratories, P.O. Box 450, Three Bridges, New Jersey 08887, and Department of Animal and Exploratory Drug Metabolism and Department of Natural Products Chemistry, Merck Sharp & Dohme Research Laboratories, P.O. Box 2000, Rahway, New Jersey 07065

Photodegradation of avermectin B_{1a} thin films under artificial light (above 260 nm) for short periods of time (greater than 60% of parent compound remaining) resulted in the formation of at least 10 primary degradates including two geometric isomers, 7 monooxygenated derivatives, and 1 dealkylated derivative. Prolonged photolysis of avermectin B_{1a} thin films (no parent compound remaining) resulted in a polar residue which appeared to consist of a complex mixture of degradates with few characteristics of the parent molecule.

INTRODUCTION

The avermectins are a class of macrocyclic lactones produced by the soil actinomycete *Streptomyces avermitilis*. They have been developed as potent, wide-spectrum agents against numerous endo- and ectoparasites in animals and man as well as against many destructive crop pests. The structural characterization (Davies and Green, 1986), mode of action, broad-spectrum efficacy in target species (Putter et al., 1981), and mammalian toxicity (Lankas and Gordon, 1989) of the avermectins have been reviewed.

Avermectin B_1 or abamectin (Figure 1), which consists of not less than 80% of the B_{1a} homologue and not more than 20% of the B_{1b} homologue, is currently experiencing rapid worldwide growth in usage as an acaricide/miticide/insecticide for a number of crops. Although abamectin is rapidly degraded on plants, limited characterization of residues has been performed (Bull et al., 1984; Iwata et al., 1985; Maynard et al., 1989a,b; Moye et al., 1990). The task of isolating and identifying degradates of avermectins in treated crops for determination of the terminal toxic residue has proven to be a significant undertaking due to the very low application rates (approximately 10 g/acre) and rapid breakdown under field-use conditions to a complex residue (Wislocki et al., 1989). The studies described in this paper examine the photolysis of avermectin B_{1a} as thin films on glass and represent the most comprehensive investigation of the environmentally induced degradation of an avermectin to date.

MATERIALS AND METHODS

Avermectin B_1 and Derivatives. Avermectin B_{1a} (B1A) was isolated from technical grade avermectin B_1 [>80% B1A and <20% avermectin B_{1b} (B1B)] obtained at Merck Sharp & Dohme Research Laboratories (MSDRL) (Rahway, NJ). The geometric isomers 8,9-(*Z*)-avermectin B_{1a} (8,9-Z) and 10,11-(*Z*)-avermectin

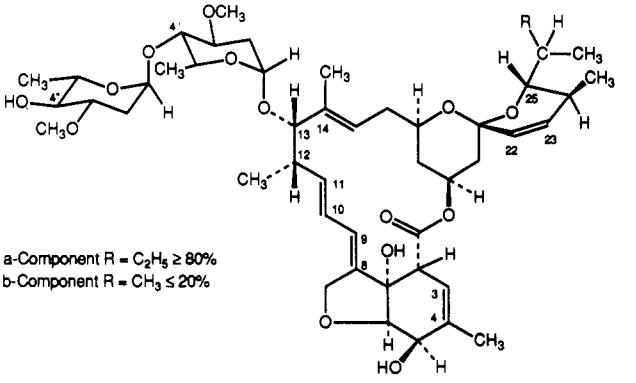

Figure 1. Structure of avermectin B_1.

B_{1a} (10,11-Z) and 8α-hydroxyavermectin B1a (8αOH) were obtained from the Department of Basic Medicinal Chemistry at MSDRL. ^{14}C-labeled B1A (labeled at C-3, C-7, C-11, C-13, and C-23; sp act. = 13.0 μCi/mg) was obtained from the Labeled Compound Synthesis Group, Department of Animal and Exploratory Drug Metabolism, MSDRL.

Photolysis of Avermectin B_{1a} Thin Films in Vitro. For B1A degradation time course studies, aliquots of a methanol solution containing highly purified [^{14}C]-B1A (sp act. approximately 1000–5000 DPM/μg) were placed in uncovered 10-mL glass beakers or glass Petri dishes (density of 0.7 μg of B1A/mm²) and dried under a stream of nitrogen at room temperature in the dark. The thin films were then placed 66 cm from a bank of 10–12 General Electric 275-W Suntanner RS bulbs in a fume hood. The surface temperature under the lights varied from 40 to 50 °C, and total surface irradiance, as measured by a black and white pyranometer (Model 8-48, Eppley Laboratories, Newport, RI), was approximately 60–70 mW/cm². The samples were removed from the light at intervals up to 48 h, and the residues were recovered by rinsing with methanol; a foil-wrapped control was placed under the lights for 48 h. For comparison to photolysis under artificial light highly purified [^{14}C]-B1A (about 10 000 dpm/μg) was applied in ethyl acetate to the wells of a Boerner slide at approximately 0.1 μg/mm², dried in the dark, and placed in sunlight for 8 h (average mW/cm² = 57; 27–35 °C), and the residues were recovered by rinsing with methanol. The residues from the thin film photolyses were assayed by HPLC as described below.

For production of primary B1A photodegradates for structural characterization, technical grade abamectin was partially purified by HPLC (to approximately 98% B1A and 2% avermectin B_{1b}), applied at a density of 0.7 μg/mm² to glass Petri dishes and photolyzed under sunlamps as above (2 h). The residues were recovered by a methanol rinse, and a total of approximately 80

* To whom correspondence should be addressed.
† Merck Sharp & Dohme, Three Bridges.
‡ Department of Animal and Exploratory Drug Metabolism, Merck Sharp & Dohme, Rahway.
§ Department of Natural Products Chemistry, Merck Sharp & Dohme, Rahway.
∥ Present address: Department of Drug Metabolism, Merck Sharp & Dohme Research Laboratories, Sumneytown Pike, West Point, PA 19486.

0021-8561/91/1439-1310$02.50/0

mg of semipurified B1A was used. Individual degradates were purified by HPLC as detailed below.

High-Pressure Liquid Chromatography of Avermectin B_{1a} Residues. *Equipment.* The HPLC equipment for analysis or purification of small amounts of B1A photodegradates consisted of a Spectra-Physics SP8700 or 8800 solvent delivery system or dual LDC Constametric pumps, a Rheodyne 7125 injector, an LDC Spectromonitor III detector, a Spectra-Physics SP8440 or Hewlett-Packard 1040A or 1040M diode array detector, a Spectra-Physics SP4200 integrator, LDC CCM, a Hewlett-Packard HP 85B or 1040M data station, and a Pharmacia Frac-100 collector. For preparative-scale HPLC an LDC Model III Constametric pump, Hewlett-Packard Model HP3394A integrator, an Isco Model 328 fraction collector, and an LDC Spectromonitor III detector with preparative-scale flow cell were used.

Analytical HPLC Methods. The total residues in the methanol rinses of B1A thin films were analyzed by using a Zorbax (7 μm, 4.6 × 250 mm), IBM (5 μm, 4.6 × 250 mm), or Axxiom (5 μm, 4.6 × 250 mm) C_{18} column eluted with methanol/water or acetonitrile/water (C_{18} HPLC). An isocratic C_{18} HPLC method (method I, elution with 85% methanol at a flow rate of 1 mL/min, Zorbax C_{18} column) was used to broadly classify and quantitate B1A residues as polar [retention times (t_R) 0–0.6 of B1A] and moderately polar (t_R approximately 0.6–0.95 of B1A), similar to previous studies of avermectin degradation in plants (Moye et al., 1990). A second C_{18} HPLC method (method II), used for assay of B1A and its photodegradates, consisted of the Zorbax C_{18} column eluted at 1.5 mL/min with methanol/water at the following proportions: 0–50 min, 79% methanol; 50–60 min, 79–100% methanol. Polar B1A residues obtained by method I from the total thin film residues were rechromatographed by a third C_{18} HPLC method (method III) using an IBM C_{18} column eluted with methanol/water (flow rate 1 mL/min) at the following compositions: 0–8 min, 30% methanol; 8–10 min, gradient to 45% methanol; 10–20 min, 45% methanol; 20–22 min, gradient to 70% methanol; 22–45 min, 70% methanol; 45–70 min, gradient to 100% methanol; 70–90 min, 100% methanol. For all three analytical C_{18} HPLC methods the eluate was monitored at 245 nm with variable-wavelength detectors or from 190 to 400 or 600 nm with the diode array detectors; fractions (0.5–1.0 min) were collected for additional HPLC or for liquid scintillation counting (LSC) in Packard Insta-Gel by using a Packard 460 or 4530 counter.

Preparative HPLC Methods. Preparative C_{18} HPLC of the total residues from photolysis of B1A thin films was performed with a Whatman Partisil Magnum C_{18} column (10-μm particle size, 20 × 500 mm) eluted with 85% methanol at a flow rate of 18 mL/min. Photodegradates isolated by preparative C_{18} HPLC of total B1A residues were typically repurified by HPLC using an Axxiom silica column (5 μm, 4.6 × 250 mm) eluted with 92% isooctane/8% ethanol at a flow rate of 3 mL/min (SI HPLC). In one instance it was necessary to resolve two photodegradates obtained from a preparative C_{18} HPLC peak by C_{18} HPLC using a Zorbax column (7 μm, 4.6 × 250 mm) eluted with 60% acetonitrile/40% water at a flow rate of 2 mL/min prior to final purification by SI HPLC. Total B1A thin film residues were also fractionated by method I for further characterization of the polar residues by method III. For all preparative methods the eluate was monitored at 245 nm with variable-wavelength detectors or from 190 to 400 or 600 nm with diode array detectors; 0.5–1.0-min fractions were collected for additional HPLC or structural analysis, and aliquots (20–50 μL) of these fractions were taken for LSC.

Pooled C_{18} HPLC fractions were dried in a Buchi rotary evaporator at approximately 30–35 °C after dilution with 9 volumes of acetonitrile; pooled SI HPLC fractions were dried at 30–35 °C under a stream of nitrogen. All purified degradates and HPLC fractions were stored at −20 °C.

Nuclear Magnetic Resonance Spectroscopy and Mass Spectrometry. Nuclear magnetic resonance spectra were obtained at 400 MHz with a Varian XL-400 spectrometer. Data were collected at room temperature in $CDCl_3$ or in $CDCl_3/C_6D_6$ mixtures by using a 1-s acquisition time and a 45° flip angle.

All FAB mass spectrometry experiments were performed by using a MAT 731 mass spectrometer with the accelerating voltage set at 8 kV. Samples were dissolved in methanol and loaded onto a probe tip coated with a 5:1 solution of dithiothreitol/dithioerythritol (magic bullet). Samples were ionized by a xenon gas FAB gun operated at 8 kV. The EI mass spectrometry experiments were performed with a MAT 212 mass spectrometer. Samples were placed in a glass crucible and vaporized by applying a linear temperature program to the probe tip from ambient temperature to 300 °C at a rate of 60 °C/min. The source temperature was set at 250 °C, and the ionization energy was 100 eV.

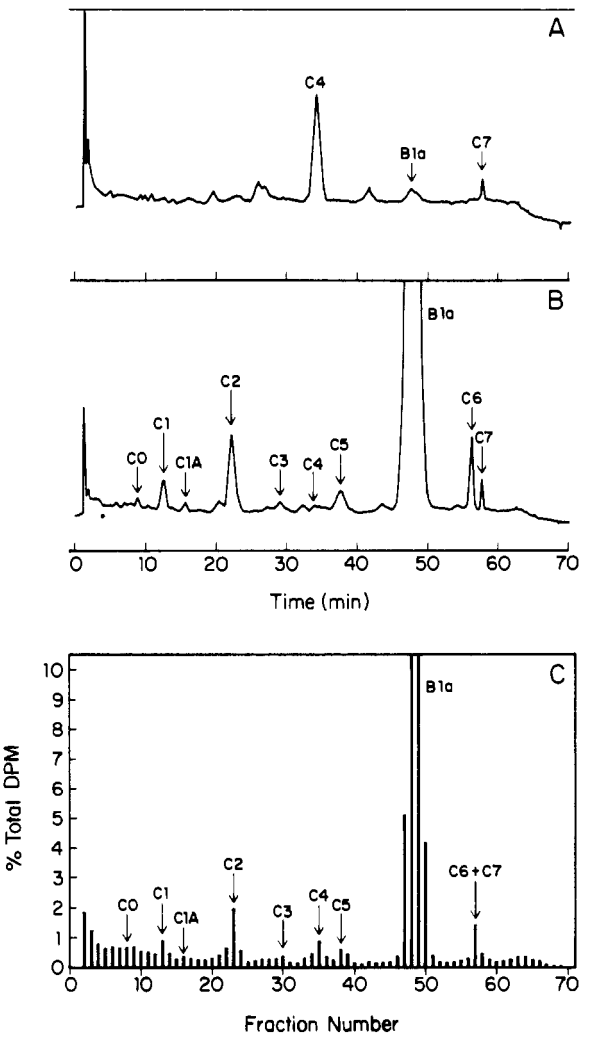

Figure 2. Analytical C_{18} HPLC (method II) of residues from photolysis of a [^{14}C]-B1A thin film for 2 h under sunlamps. (A) 280-nm absorbance; (B) 245-nm absorbance; (C) radioprofile.

UV Spectra of B1A Thin Film vs B1A Solution. Purified avermectin B1A was applied in ethyl acetate to one interior side of a quartz cuvette and dried to give a thin film of approximately 0.5 μg/mm^2. The UV spectrum of the B1A thin film was measured from 200 to 700 nm vs an empty cuvette in a Perkin-Elmer Model 320 spectrophotometer, and then the thin film was solubilized with methanol and the spectrum recorded again vs methanol over the same wavelengths.

RESULTS

Primary Photodegradates of Avermectin B_{1a}. *Chromatography.* The C_{18} HPLC chromatograms of residues (approximately 50 μg) obtained after a 2-h photolysis of highly purified [^{14}C]-B1A under sunlamps indicate the presence of multiple photodegradates (Figure 2). The UV absorbance profile at 245 nm has five major peaks (C1, C2, C5, C6, and B1A) as well as five minor peaks (C0, C1A, C3, C4, and C7); other minor peaks are apparent (Figure 2B). The diene functionality of B1A (Figure 1) has an absorbance maximum at 243 nm (ϵ = 31.85 mM^{-1}) and therefore degradates in peaks C0–C7 apparently have an intact diene. The UV absorbance profile at 280 nm (Figure

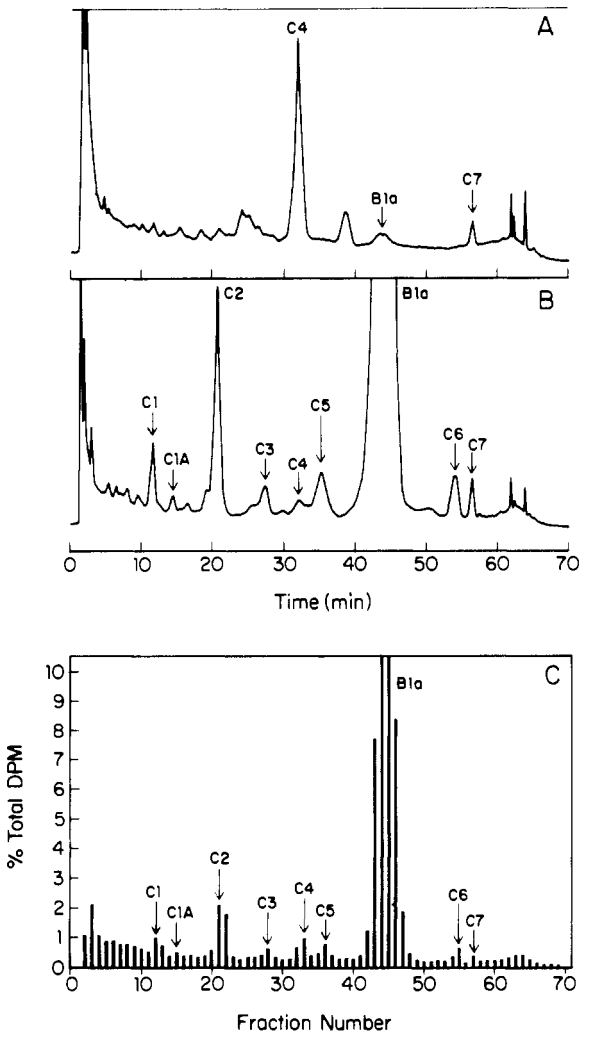

Figure 3. Analytical C_{18} HPLC (method II) of residues from photolysis of a [^{14}C]-B1A thin film for 8 h in sunlight. (A) 280-nm absorbance; (B) 245-nm absorbance; (C) radioprofile.

2A) has one major (C4) and two minor (B1A, C7) peaks coeluting with peaks of 245-nm absorbance (Figure 2B) in addition to several other minor peaks that do not coelute with 245-nm peaks. Peaks of radioactivity (Figure 2C) corresponding to the indicated UV peaks (Figure 2A,B) are apparent except for C7, which was not resolved from C6 by collecting 1-min fractions of eluate. Considerable background radioactivity relative to peak height is apparent with most of those degradates eluting earlier than C2, and this background radioactivity probably represents multiple minor degradates; a considerable fraction of radioactivity with little absorbance at 245 or 280 nm elutes before 10 min (Figure 2). Photolysis of a thin film (approximately 0.1 μg/mm^2) of highly purified [^{14}C]-B1A for 8 h in sunlight and C_{18} HPLC of the total residues as above for sunlamp-photolyzed material resulted in UV profiles (245 and 280 nm) and a radioprofile (Figure 3) essentially identical with that obtained for the sunlamp-photolyzed material as in Figure 2. Preparative C_{18} HPLC of residues (40 mg total) from photolysis of a B1A thin film (0.7 μg/mm^2, approximately 98% B1A and 2% B1B) for 2 h under sunlamps resulted in six major peaks with absorbance at 245 nm (P0–P4, Figure 4) in addition to B1A and a number of minor peaks. Analytical C_{18} HPLC of these same residues (100 μg) gave a 245-nm profile essentially identical with that obtained with photolysis of highly purified [^{14}C]-B1A (Figure 2) except for an additional peak partially coeluting with C4 which is B1B

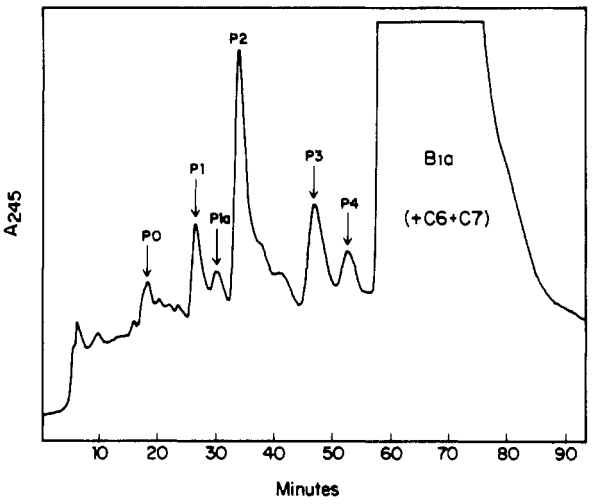

Figure 4. Preparative C_{18} HPLC of residues from photolysis of a B1A (98% B1A, 2% B1B) thin film for 2 h under sunlamps. Material equivalent to 40 mg of B1A was chromatographed.

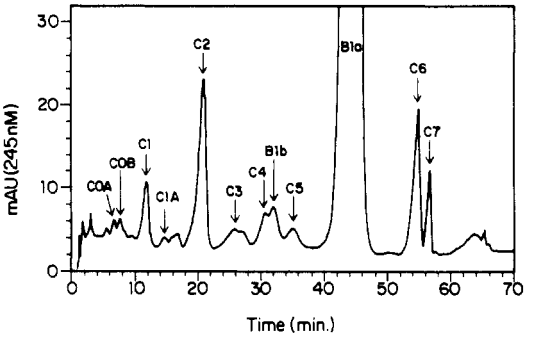

Figure 5. Analytical C_{18} HPLC (method II) of total B1A thin film residues subjected to preparative C_{18} HPLC as in Figure 3. Material equivalent to 100 μg of B1A was chromatographed.

Table I. HPLC Analyses of Residues from Photolysis of an Avermectin B_{1a} Thin Film (0.7 μg/mm^2) after Preparative C_{18} HPLC

prep C_{18} HPLC peak[a]	major SI HPLC peaks[b]	anal. C_{18} HPLC peaks[c]	photodegradate designation
P0	1.52	C0A	C0A
	2.02	C0B	C0B
P1	1.34	C1	C1
P1A	1.31	C1A	C1A
P2	1.30	C2	C2
P3	0.83	C4	C4A, B[d]
	1.00	B1B	B1B[e]
	1.76	C5	C5A
	2.33	C5	C5B
P4	0.83	C4	C4A, B[d]
	1.00	B1A	B1A
	1.76	C5	C5A
	2.33	C5	C5B

[a] See Figure 4. [b] Selectivity relative to B1A. [c] See Figure 5. [d] Separated by C_{18} HPLC as in Figure 6. [e] Avermectin B_{1b} is not a photodegradate of avermectin B_{1a}.

(Figure 5); C0A and C0B result from partial resolution of C0 not apparent in Figure 2. Fractions corresponding to peaks P0, P1, P1A, P2, P3, and P4 from two preparative C_{18} HPLC runs (80 mg total material) were pooled, dried, and fractionated by SI HPLC, and the major SI HPLC peaks were collected and assayed by C_{18} HPLC method II. Table I summarizes the results of successive HPLC fractionations of B1A photodegradates obtained after a 2-h photolysis of a thin film. Preparative C_{18} HPLC peaks P1, P1A, and P2 (Figure 4) appeared to contain mostly a single component after SI HPLC and analytical C_{18} HPLC (Table I); these photodegradates corresponding to C1, C1A,

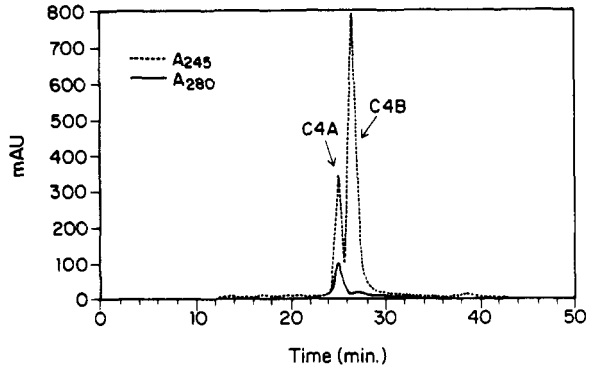

Figure 6. Resolution of C4 (Figures 1 and 5) by C_{18} HPLC. Column (Zorbax) was eluted with 60% CH_3CN/40% H_2O at a flow rate of 2 mL/min.

and C2, respectively, in Figure 5 were analyzed by NMR and/or FAB or EI-MS after purification by SI HPLC. Preparative C_{18} HPLC peak P0 (Figure 4) was resolved into two major components when subjected to SI HPLC (Table I); these two photodegradates corresponded to C0A and C0B on the analytical C_{18} HPLC system (Figure 5) and were analyzed by NMR and/or FAB or EI-MS after purification by SI HPLC. Preparative C_{18} HPLC peak P3 was resolved into four peaks by SI HPLC (Table I); two of these SI HPLC peaks (C5A,B) coeluted with C5 on the analytical C_{18} HPLC system (Table I; Figure 5), one SI HPLC peak coeluted with B1B on the analytical C_{18} HPLC system (Table I; Figure 5), and one SI HPLC peak coeluted with C4 on the analytical C_{18} HPLC system (Table I; Figure 5). Preparative C_{18} HPLC peak P4 was also resolved into four peaks by SI HPLC similar to peak P3, but the peak coeluting with B1A standard was B1A rather than B1B (Table I; Figure 5). Close inspection of SI HPLC or analytical C_{18} HPLC (method II) UV profiles of B1A photodegradates from preparative C_{18} HPLC peaks P3 and P4 at 245 and 280 nm indicated that at least two components were present as the peak absorbances at the two wavelengths were very slightly resolved (data not shown). The two components of C4 were resolved by C_{18} HPLC using acetonitrile rather than methanol (C4A,B, Figure 6) and then repurified by SI HPLC prior to NMR and FAB/EI-MS; C4A contributes essentially all of the 280-nm absorbance associated with C4 (Figures 2A and 6).

Photodegradate C5A (Table III) cochromatographed with standard 8aOH by C_{18} HPLC method II and by SI HPLC; photodegradate C4B (Table III) cochromatographed with standard 10,11-Z by the same two HPLC methods (data not shown). Photodegradate C6 from either sunlamp- or sunlight-photolyzed thin films of [^{14}C]-B1A coeluted with standard 8,9-Z by C_{18} HPLC method II (data not shown). When C6 was isolated from [^{14}C]-B1A thin film residues by C_{18} HPLC and rechromatographed by SI HPLC, coelution with standard 8,9-Z was also observed (data not shown).

The photodegradates corresponding to C3 (Figures 3 and 5) apparently were contained in the two shoulders on P2 of the preparative C_{18} HPLC of thin film residues (Figure 4); when these preparative C_{18} HPLC fractions were dried and rechromatographed on a Zorbax semi-preparative C_{18} column (7 μm, 10 × 250 mm), peaks (A245) corresponding to C2 and C3 were observed (data not shown). When the C3 fractions from the semipreparative C_{18} HPLC were dried and rechromatographed by SI HPLC, essentially no peaks (A245) were observed (data not shown), indicating instability or strong retention on the silica column; no further attempts to isolate these photodegradates were made.

Mass Spectroscopy. The FAB and/or EI-MS of nine B1A photodegradates and B1B isolated from residues formed after photolysis of a B1A thin film (98% B1A/2% B1B) for 2 h as described above are summarized in Table II and compared with the known EI-MS ions for B1A (Albers-Schonberg et al., 1981). Five photodegradates (C0A, C0B, C1, C1A, and C2) have increased by 16 mass units at C13–C16 as indicated by FAB MS of the parent ion (888 vs 872 for B1A), the appearance of an m/z ion of 321 (vs 305 for B1A at C13–C26), and the presence of an m/z ion of 221 (C17–C26) in both B1A and each photodegradate (Table II). Photodegradate C5A has increased by 16 mass units at C1–C12 as suggested by FAB MS (888 vs 872 for B1A), the appearance of an m/z ion of 582 (vs 566 for B1A at C1–C26), and the presence of an m/z ion of 305 (C13–C26) in both B1A and C5A (Table II). Photodegradate C5B has lost 14 mass units on the terminal sugar as suggested by the FAB MS (858 vs 872 for B1A), the appearance of an m/z ion of 131 (vs 145 for B1A at C″1–C″5), and the lack of changes to the macrolide ring (Table II). Photodegradate C4A has gained 14 mass units at C1–C12 as indicated by the appearance of an m/z ion of 580 (vs 566 for B1A at C1–C26) and the presence of an m/z ion of 305 (C13–C26) in both B1A and C4B (Table II). Finally, photodegradate C4B was unchanged relative to B1A as indicated by FAB and EI-MS (Table II). Photodegradate C6 was not analyzed by MS.

NMR Spectroscopy. The 14-hydroxy-Δ^{15} analogue of B1A is proposed as a reasonable possibility for C1 on the basis of the upfield displacement of the 14-methyl to 1.36 ppm and the appearance of additional peaks between 5.6 and 5.8 ppm (in $CDCl_3$) which are interpretable as a pair of *trans*-vinyl protons. Two lines, in a clear region, separated by 15 Hz at 5.60 and 5.64 could represent one of the *trans*-vinyl protons and would be assigned to H-15 since there is no resolved secondary splitting. On the basis of the relative intensity of the two peaks, its neighbor would be located within the complex multiplet centered at 5.72 ppm composed of H-10 or H-11 and H-23. Four lines, consistent with a double doublet with the larger peak separation, can indeed be discerned in this cluster. Unfortunately, a crucial double-irradiation experiment which could have confirmed the assignment was precluded by sample degradation. The NMR spectrum of C2 is shown in Figure 7. Key NMR observations (in $CDCl_3$) were the absence of a 14-methyl peak and the presence of a novel doublet at 4.46 ppm (J = 10.5 Hz) and a terminal methylene. The terminal methylene was identified in a $CDCl_3/C_6D_6$ solvent mixture which gave better resolution in the low-field region (Figure 7). Strong circumstantial evidence that the 4.46 ppm doublet (in $CDCl_3$) was a displaced H-15 was provided by a double-irradiation experiment in which both H-17 and the 4.46 ppm doublet were affected when the irradiation frequency was set at 1.5 ppm. This implied that the irradiated proton was a neighbor of both protons, i.e., H-16. The C4A residue was assigned as the 8α-lactone on the basis of the absence of the 8α-CH_2 resonance and the close correspondence of key signals with those of an authentic specimen. These include H9 (6.62 ppm), H10 (9.25 ppm), H5 (4.49 ppm), and the 4-CH_3 (1.96 ppm), all of which were displaced downfield from B1A. The C4B and C6 residues were determined to be the 10,11-Z and 8,9-Z geometric isomers of B1A, respectively, after comparison to NMR of authentic specimens. The NMR spectrum of C5B indicated a close resemblance to B1A except for the presence of only one

Table II. FAB/EI-MS of B1A Photodegradates and B1B Isolated from Residues Obtained by Photolysis of an Avermectin B_{1a} (Containing 2% B1B) Thin Film (0.7 $\mu g/mm^2$) for 2 h

	m/z ion for indicated compound										
carbon no.	B1A	B1B	C0A	C0B	C1	C1A	C2	C4A	C4B	C5A	C5B
1″–5″	145	145	145	145	145	145	145	145	145	145	131
1–26	566	552	582	582	582	582	582	580	566	582	566
13–26	305	291	321	321	321	321	321	305	305	305	305
17–26	221	207	221	221	221	221	221	221	221	221	221
FAB MS	872	858	888	888	888	888	888	nd[a]	872	888	858

[a] nd, not determined.

Table III. Criteria for Structural Assignment of Primary Avermectin B_{1a} Photodegradates

photodegradate	NMR	MS	UV spectrum[a]	HPLC[a]
C0A (14- or 15-OH?, Δ?-B1A)	–	+	–	–
C0B (14- or 15-OH?, Δ?-B1A)	–	+	–	–
C1A (14- or 15-OH?, Δ?-B1A)	–	+	–	–
C1 (14-OH, Δ^{15}-B1A)	+	+	–	–
C2 (15-OH, 14-*exo*-methylene-B1A)	+	+	–	–
C4A (8α-oxo-B1A)	+	+	–	–
C4B (10,11-Z-B1A)	+	+	+	+
C5A (8α-OH-B1A)	–	+	+	+
C5B (3″-*O*-demethyl-B1A)	+	+	–	+
C6 (8,9-Z-B1A)	–	+	+	+

[a] Compared with authentic standard.

methoxyl peak and was assigned as the 3″-*O*-demethyl analogue. The NMR spectrum of the C5A residue was not obtained.

Structure and UV Spectra. The proposed structures of seven primary photodegradates of B1A are illustrated in Figure 8, and the data used for structural assignment are summarized in Table III. A comparison of the diode array spectra obtained during SI HPLC of 8,9-Z standard and photodegradate C6 (Figure 9A) and 8aOH standard and photodegradate C5A (Figure 9B) indicates identity of the degradates with respective standards. The diode array spectra of 10,11-Z standard (Figure 9C) and photodegradate C4B during SI HPLC are also identical (data not shown). The diode array spectrum of photodegradate C7 (Figure 9D) taken during C_{18} HPLC of [^{14}C]-B1A thin film residues (Figure 2) is compared with that of B1A; a smoothing and blue shift of the major UV peak and appearance of a second UV peak centered around 280 nm distinguish this compound from the parent. A comparison of the diode array spectrum of standard B1A vs spectra of photodegradates C0A, C0B, C1, C1A, C2, C4A, and C5B during SI HPLC is made in Figure 10; photodegradates C0B (Figure 10B) and C5B (Figure 10G) have spectra identical with B1A.

The diene of B1A appears to serve in general as a "reporter" group when its UV spectrum is compared to those of the primary photodegradates. Alterations of B1A involving conformational changes in the macrolide ring system (C1, C2, C4B, and C6, Figure 8) or conjugation with the diene (C4A and C5A, Figure 8) were evidenced by changes in the UV spectra (Figures 9 and 10), whereas alterations at positions outside the macrolide (C5B, Figures 8 and 10G) were not. Avermectin B_{1b}, differing from B1A by a methylene at the R group of C26 (Figure 1), has a UV spectrum identical with that of B1A (data not shown).

The UV spectrum of C7 (Figure 9D) is suggestive of both a conformational change at the diene and conjugation with the diene, but this photodegradate was not characterized further. Photodegradates C0A, C0B, and C1A have resulted from oxygen addition to B1A at C13–C16 (Table II), and only the spectrum of C0B is unaltered relative to that of B1A (Figure 10A,B,D).

Time Course Studies. The relative contributions of B1A and its photodegradates C2 (14-*exo*-methylene-15-OH-B1A), C3 (unknown), C4 (8α-oxo-B1A + 10,11-Z), C5 (8αOH + 3″-*O*-demethyl-B1A), and C6 (8,9-Z) to the total ^{14}C residue during photolysis (sunlamp) of a highly purified thin film (0.7 $\mu g/mm^2$) of [^{14}C]-B1A for 1–24 h as assayed by C_{18} HPLC method II are indicated in Figure 11; these photodegradates were present at essentially constant levels until the parent compound was completely degraded. Individual photodegradates in C4 and C5 were not quantitated. Photodegradates eluting before C2 (C0A, C0B, C1, C1A) could not be accurately quantitated after 2 h of photolysis due to high background radioactivity (data not shown). The first-order half-life of B1A was approximately 2–3 h under these conditions (average of two experiments). Recovery of ^{14}C after photolysis of B1A thin films for 1–48 h under sunlamps was essentially quantitative (about 90% or above at all time points for two separate experiments); a dark control (foil-wrapped) placed among light-exposed samples in one experiment was approximately 90% B1A after 48 h.

The criteria for complete or partial structural assignment of primary B1A photodegradates are summarized in Table III.

Terminal Photodegradates of Avermectin B_{1a}. *Time Course Studies.* The C_{18} HPLC (method I) radioprofiles of [^{14}C]-B1A thin film residues at 2–48 h of photolysis (sunlamp) are represented in Figure 12; B1A elutes at approximately 20–22 min. The arbitrary designation of polar ($t_R \leq 0.6$ of B1A), moderately polar (t_R between 0.6 and 0.95 of B1A), and nonpolar ($t_R >$ B1A) residues (Figure 12B) is similar to that in previous plant metabolism studies (Moye et al., 1990). The polar residues contribute approximately 80% or greater to the total ^{14}C residue when the parent compound is approximately 10% or less of the total residue with the remainder split approximately equally between moderately polar and nonpolar residues (data not shown). The primary B1A photodegradates (Table III) elute in the following manner under the conditions of C_{18} HPLC method I: C0A, C0B, C1, C1A, C2, polar; C3, C4 (A + B), C5 (A + B), moderately polar; C6 and C7 elute after B1A (data not shown). There appeared to be little change in the radioprofile from 22 to 48 h of photolysis (Figure 12C,D).

When polar residues from photolysis of [^{14}C]-B1A thin films (Figure 12) were isolated from the total [^{14}C]-B1A residues after 2–48 h of photolysis by C_{18} HPLC method I and rechromatographed by step gradient C_{18} HPLC (method III), four regions of radioactivity corresponding to the four steps of the gradient were observed at earlier time points (2–10 h), while only three peaks of radioactivity were observed at 22 or 48 h of photolysis (Figure 13). There was an increase in early-eluting polar residues with time of photolysis from 2 to 22 h (Figure 13); as with the total ^{14}C residues (Figure 12), however, little change in radio-

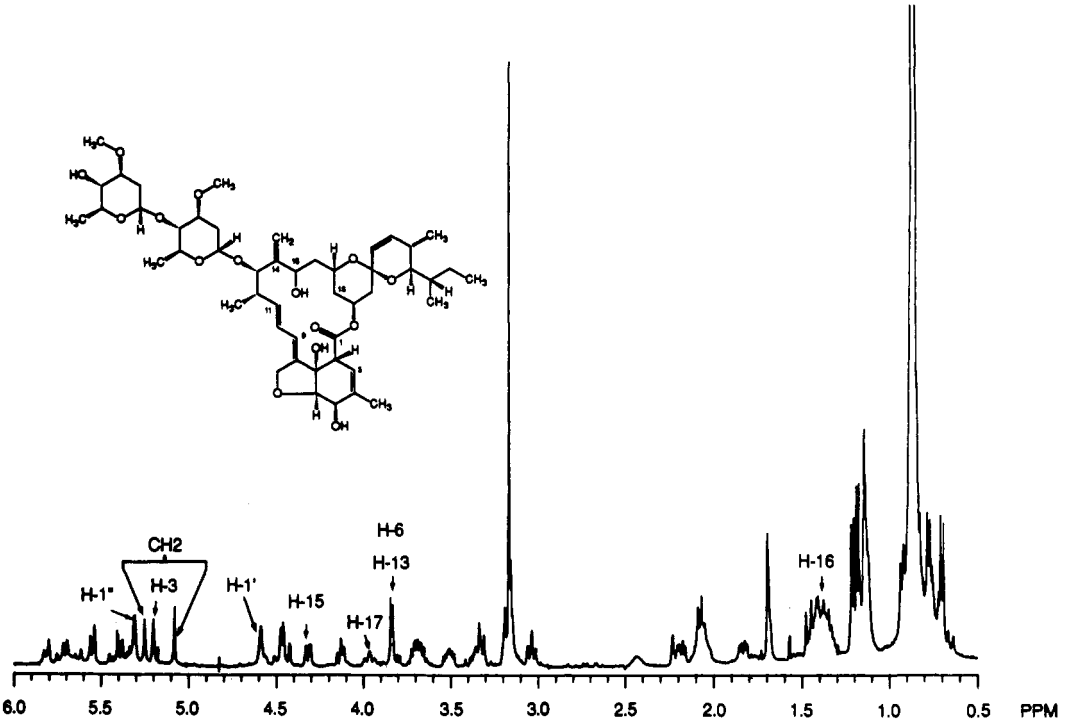

Figure 7. Proton NMR of C2 photodegradate of B1A at 400 MHz in ($CDCl_3/C_6D_6$).

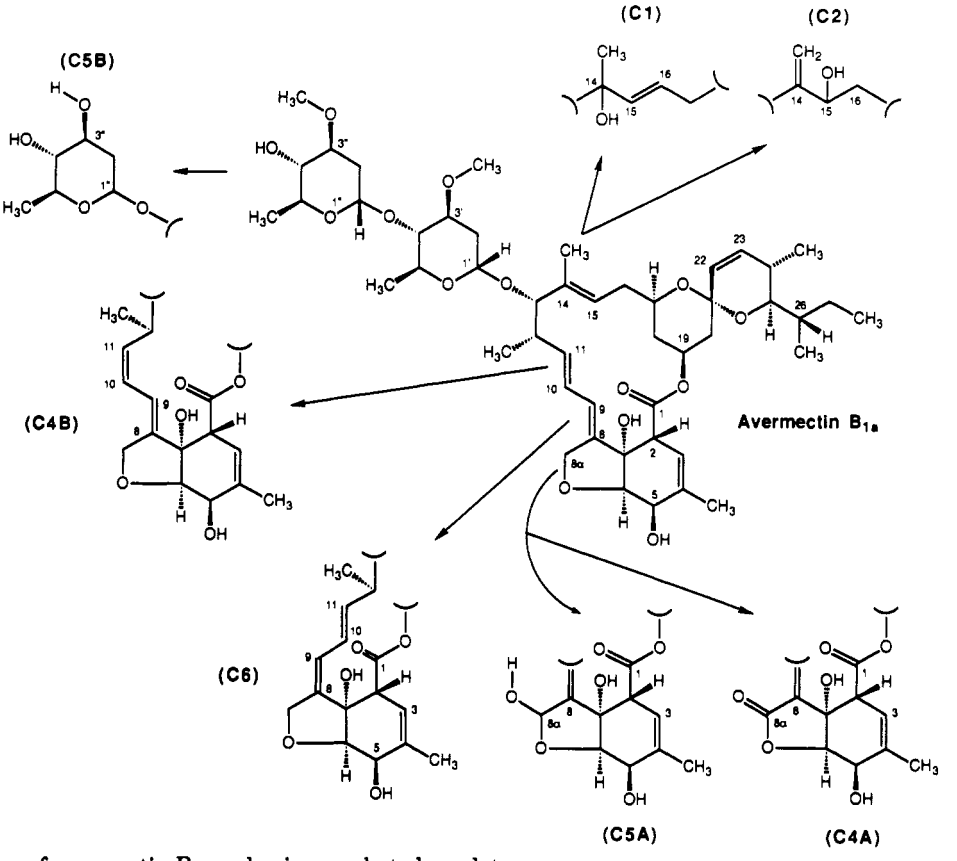

Figure 8. Structures of avermectin B_{1a} and primary photodegradates.

profile was observed from 22 to 48 h (Figure 13). The polar ^{14}C residues eluting in the last portion of the step gradient contained the primary photodegradates C0A, C0B, C1, C1A, and C2 (Figure 13, 2 and 5 h; Table III) in addition to several minor peaks with 245-nm absorbance (data not shown). Numerous other chromatography systems were tried in an effort to resolve the polar B1A residues present at extended periods of photolysis (when B1A is completely degraded) with little success (data not shown). The step gradient method (method III) has proven useful for comparison of radiolabeled polar B1A residues from various sources, conditions, etc. by subdivision into four polarity classes.

UV Spectroscopy and Mass Spectrometry. Diode array spectra (Figure 9E) taken at various points of the single peak of polar [^{14}C]-B1A residues observed during isocratic C_{18} HPLC analysis (Figure 12C) have mostly end absorbance and lack a distinctive peak between 240 and 280 nm

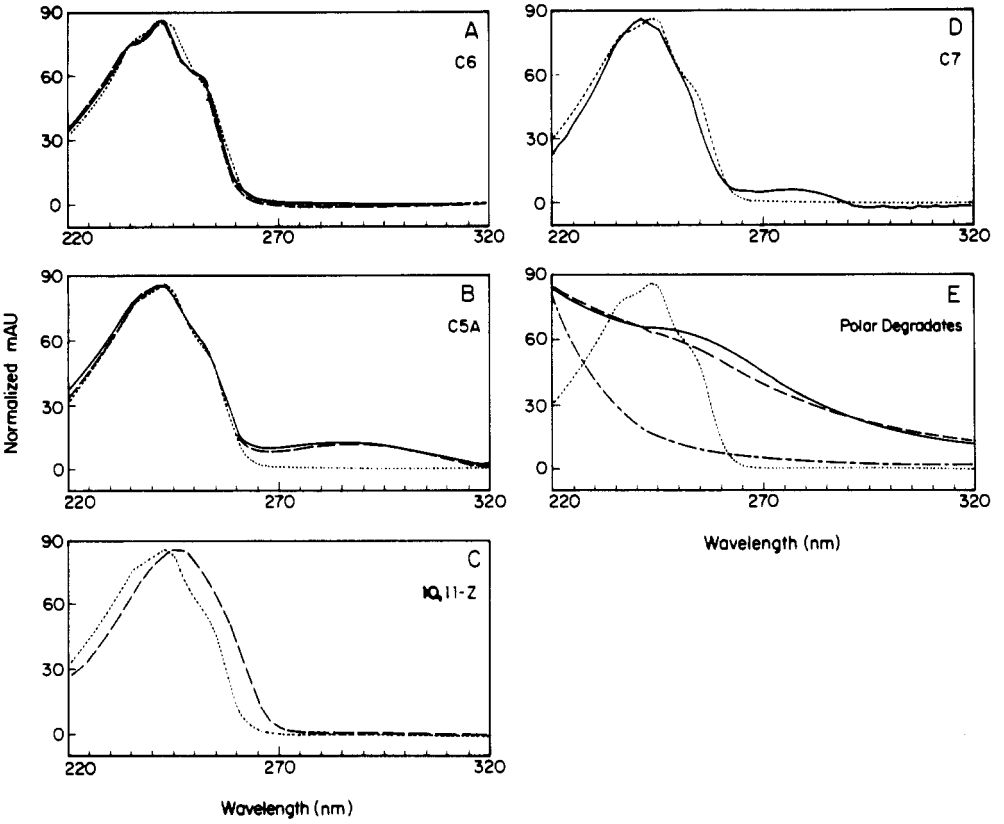

Figure 9. Comparison of diode array spectra of B1A (···) and (A) 8,9-Z standard (- - -) and C6 (—); (B) 8αOH standard (- - -) and C5A (—); (C) 10,11-Z standard (- - -); (D) C7 (—). (E) Polar degradates at leading midpoint (—), apex (- - -), and trailing midpoint (– - –) of peak in Figure 12C.

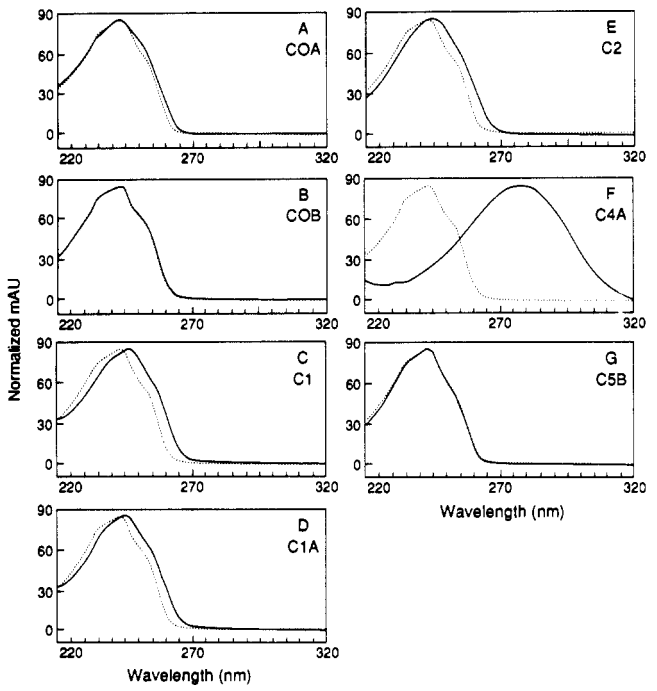

Figure 10. Comparison of diode array spectra of B1A standard (···) and (A–G) indicated B1A photodegradates (—).

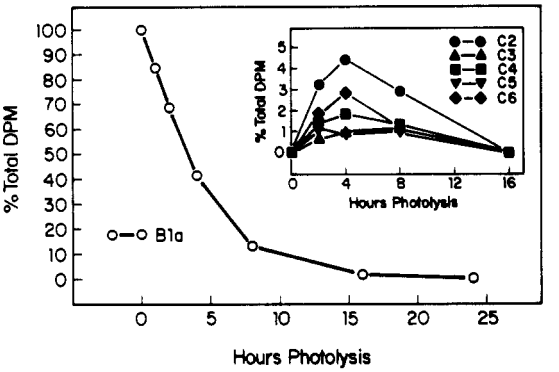

Figure 11. Time course of B1A degradation and primary photodegradates profile during photolysis of a [^{14}C]-B1A thin film under sunlamps. Values expressed as percent contribution to total DPM recovered from HPLC column (method II).

characteristic of the parent and its primary photodegradates (Figures 9 and 10).

The polar residues from photolysis of a [^{14}C]-B1A thin film for 22 h were subjected to C_{18} HPLC method III (Figure 13), and fractions of eluate were examined by CI-MS under conditions such that only the B1A parent ion would be detected from a B1A standard (i.e., no fragmentation). Under these CI-MS conditions numerous species of about half of the mass of B1A or less were seen, but no structural assignments could be made (data not shown).

UV Spectrum of Avermectin B_{1a} Thin Film vs Solution. The UV spectrum of a B1A thin film on quartz glass (0.5 μg/mm^2) and that of B1A in methanol (66 μg/mL) were identical with that of its diode array spectrum (Figure 9) which indicates little absorption above 270 nm. No absorption of light was observed between 320 and 700 nm for B1A in a thin film or in methanol (data not shown).

DISCUSSION

The observed photolability of avermectin B_{1a} in the presence of oxygen and the apparent complexity of the resultant degradates may be rationalized by the abundance of potentially oxygen-sensitive sites (three double bonds at carbons 3–4, 14–15, and 22–23; a diene at carbons 8–11; ether linkages at the 3-position of each oleandrosyl residue

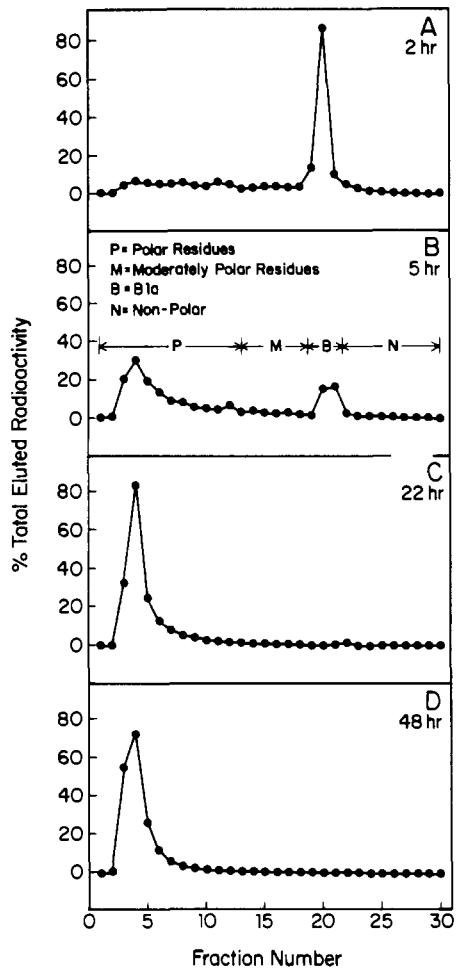

Figure 12. C_{18} HPLC (method I) radioprofile of [^{14}C]-B1A thin film residues after 2–48 h of photolysis under sunlamps (A–D). Polar (t_R < 0.6 of B1A), moderately polar (t_R between 0.6 and 0.95 of B1A), and nonpolar residues are indicated in (B).

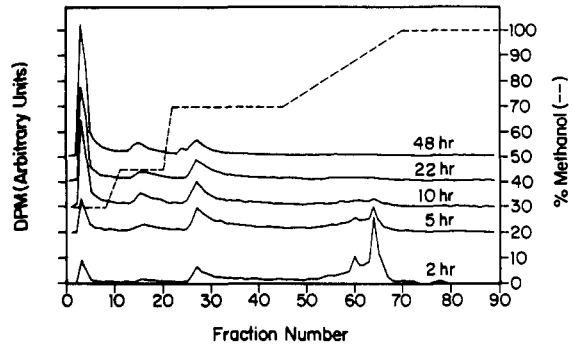

Figure 13. C_{18} HPLC (method III) radioprofile of polar residues (Figure 12) after 2–48 h of photolysis under sunlamps.

as well as at C6–C8a). The apparent lack of absorbance of B1A thin films within the wavelength range (290 nm and above) of sunlight or simulated sunlight, however, seemingly precludes direct photolysis as a mechanism of B1A photodegradation. The 8α-oxo-B1A and 8αOH photodegradates, however, do absorb light above 290 nm (Figures 8 and 10) and may degrade by direct photolysis. Nevertheless, the photolability of avermectin B_{1a} thin films, combined with the property of tight soil binding, assures that no accumulation occurs in the environment.

Primary Photodegradates of Avermectin B_{1a}. The C4A and C5A photodegradates (Figure 8) are formed by oxygen addition to the 8α- position of B1A, possibly by a radical reaction with O_2 forming an initial hydroperoxide. The C-8α position may be especially prone to radical reactions since it is both allylic and α to an ether linkage (Fisher and Mrozik, 1989); the 8α-hydroperoxide has been isolated as an impurity in avermectin syntheses (Fisher and Mrozik, 1989). The ketone (C4A) and hydroxy (C5A) functionalities could arise from the hydroperoxide by loss of water and photolytic cleavage, respectively. Conjugation between the ketone at C-8α of C4A and the diene results in the shift of absorbance maximum to 280 nm (Figure 10F). The broad UV absorbance of C5A centered at approximately 285 nm (Figure 9B), in addition to the 243-nm peak, apparently results from the equilibrium mixture of the ring-opened aldehyde and hemiacetal (Bull et al., 1984). Formation of a hydroperoxide at the 3″-*O*-methyl (similar to the 8α-hydroperoxide) followed by cleavage of the hydroperoxide and loss of formaldehyde could result in C5B (Figure 8); no analogous 3′-*O*-demethyl product, however, was found. The C5B product has also been reported as a metabolite (Miwa et al., 1982).

The insertion of oxygen at carbons 14 (C1) and 15 (C2) of B1A with the accompanying double-bond shifts is consistent with formation of an allylic hydroperoxide from singlet oxygen by the ene-type reaction (Foote, 1971) followed by cleavage to the observed hydroxyl (Figure 8). The source of singlet oxygen under these conditions, however, is unknown. Photodegradates C0A and C1A could also result from reaction of singlet oxygen with the 14,15 double bond via the ene reaction as FAB MS fragmentation indicates incorporation of O at carbons 13–16 (Table II) and the diene spectra are altered relative to that of B1A (Figure 10A,D), consistent with a shifted double bond as for C1 and C2 (Figure 10C,E). The C0B product also has undergone addition of oxygen at carbons 13–16 (Table II), but no change in UV spectra is observed (Figure 10B); this photodegradate, therefore, may form by a radical mechanism with no allylic shift of the 14,15 bond. The low yield of C0A, C0B, and C1A from thin film photolysis (approximately 0.03%) precluded NMR analysis. The 14,15 double bond region of B1A appears, therefore, to be the region most sensitive to initial photooxidation as the five primary photodegradates at carbons 13–16 (C0A, C0B, C1, C1A, and C2) contribute the largest proportion to B1A degradates as indicated by the non-B1A radioactivity in Figure 2C. Alternatively, the primary photodegradates resulting from oxygen addition at carbons 13–16 may be more stable under the photolysis conditions than other primary photodegradates.

The geometric isomers at the 10,11 (C4B) and 8,9 (C6) double bonds have been reported as photoproducts of B1A in solution (Mrozik et al., 1988); C6 has been described as a degradate in plants (Moye et al., 1990; Maynard and Maynard, 1989). The UV spectra of C4B (exactly as 10,11-Z standard in Figure 9C) and C6 (Figure 9A) reflect diene alterations relative to B1A consistent with previous studies (Maynard and Maynard, 1989; Moye et al., 1990). The presence of the 8,9-Z analogue after exposure of B1A to sunlight observed in the present studies and previously by others (Moye et al., 1990) is interesting since this photoisomer would apparently require 220–270-nm light for formation. Recent photoisomerization studies (O'Shea and Foote, 1988) of 2,4-hexadiene in solution in the presence of a sensitizer strongly suggest singlet oxygen involvement in intraconversion of the *E,E*, *E,Z*, and *Z,Z* forms. Whether isomerization of B1A in thin films exposed to sunlight is caused by a weak absorption at 290 nm or above or involves singlet oxygen is unknown; the conditions (N_2 atmosphere) under which photoisomerization of B1A in cyclohexane was observed (Mrozik et al., 1988) indicate that direct absorption of light caused the isomerization.

Since all diene UV absorbance is eventually lost during photolysis of B1A (Figure 9E), this substructure must undergo reactions other than cis–trans isomerizations; primary photoproducts resulting from oxygen addition in the diene region would cause the observed loss of UV absorbance, although these products have not been isolated.

The remarkable similarity of C_{18} HPLC UV and radioprofiles of B1A photodegradates obtained by photolysis of thin films under sunlamps (Figure 2) or in sunlight (Figure 3) indicates that photolysis studies of B1A conducted under these artificial lighting conditions can reasonably be extrapolated to what would occur environmentally. While structural determinations of primary B1A photodegradates formed in vitro in natural sunlight were not performed, the similarity of C_{18} HPLC chromatograms of sunlight and sunlamp B1A residues are consistent with the very minor spectral output of the sunlamps below 290 nm (as determined by spectroradiometer, data not shown).

Terminal Photodegradates of Avermectin B_{1a}. Extended photolysis of B1A (little or no parent remaining) results in a polar residue as evidenced by lack of retention on reverse-phase HPLC (Figure 12). Little information has been obtained as to the identity of these end products of B1A photooxidation since efforts to obtain purified residue components by HPLC techniques have not been successful. Derivatization of terminal B1A residues followed by GC/MS or HPLC/MS or fractionation of underivatized residues by gel permeation HPLC may be useful for detection or isolation of fragments produced by photooxidative processes. Interestingly, very little loss of radiolabel was observed by 48 h of photolysis, suggesting that few volatile fragments were produced under these conditions. Previous studies of [^{14}C/^{3}H]-B1A degradation on citrus fruit and after photolysis on glass for 6 days (Maynard et al., 1989a, b) have indicated that volatile residues do occur; although little change in the C_{18} HPLC radioprofile of [^{14}C]-B1A residues from 22 to 48 h of photolysis was observed (Figures 12 and 13), it may be possible that the terminal residues observed in the present studies slowly photodegrade to more volatile products.

The progression from primary to terminal B1A photodegradates likely involves numerous intermediates. For example, we have demonstrated nine primary photodegradates at five regions of the B1A molecule: carbons 13–16 (4), 3″ (1), 8α (2), and 8,9 (1) and 10,11 (1) double bonds. Assuming that alteration at one or more of the five known sites would not preclude alterations at the other sites (with the exception of the 8,9-Z and 10,11-Z isomers), approximately 100 combinations of 2–4 changes in the B1A molecule are possible with an intact macrolide; if other primary B1A photodegradates are found, this would considerably increase the number of possible combinations. Although no secondary, tertiary, or quaternary photodegradates were demonstrated in the present studies, other investigators, using the technique of ^{252}Cf ionization mass spectrometry, have detected species in the total residue from photolysis of B1A thin films which have up to five additional oxygens relative to the parent compound (J. MacConnell, personal communication). The synthesis of large quantities of primary B1A photodegradates and derivatives of B1A with one or more selectively reduced double bonds for use in future photolysis studies will hopefully increase our understanding of the mechanisms involved in the photodegradation of avermectins.

Clearly, then, isolation and identification of intermediate and terminal avermectin B_{1a} photodegradates obtained in vitro will likely be a challenging problem in view of the complex pathways available for degradation. Whether similar degradation of avermectin B_{1a} occurs in plants could be inferred by demonstration of primary photodegradates as obtained in vitro soon after application of the pesticide. More extensive photodegradation of B1A occurs in crops at typical preharvest intervals of several days to several weeks (Moye et al., 1990). Isolation and structural characterization of terminal B1A photodegradates from crops, however, will certainly present additional obstacles beyond that of the inherent complexity of B1A photodegradation such as incorporation into natural products (Feely and Wislocki, 1991), loss of residue (Maynard et al., 1989a; Moye et al., 1990), or metabolism. Furthermore, the toxicity of polar B1A degradates, when tested as an aggregate derived from photolysis in vitro (Wislocki et al., 1989; Crouch et al., unpublished results) or from field-grown citrus fruit (Crouch et al., unpublished results), has been found to be negative at the highest levels tested, obviating the need for characterization of plant residues that would not present a hazard to human health.

ACKNOWLEDGMENT

The efforts of the Labeled Compound Synthesis Group, Department of Animal and Exploratory Drug Metabolism, MSDRL, are earnestly appreciated.

ABBREVIATIONS USED

B1A, avermectin B_{1a}; C_{18} HPLC, high-pressure liquid chromatography with octadecyl bonded phase; CI, chemical ionization; EI, electrical ionization; FAB, fast atom bombardment; HPLC, high-pressure liquid chromatography; MS, mass spectrometry; NMR, nuclear magnetic resonance; SI HPLC, high-pressure liquid chromatography with silica; UV, ultraviolet; 8,9-Z, 8,9-(*Z*)-avermectin B_{1a}; 10,11-Z, 10,11-(*Z*)-avermectin B_{1a}, 8αOH, 8α-hydroxyavermectin B_{1a}.

LITERATURE CITED

Albers-Schonberg, G.; Arison, B. H.; Chabala, J. C.; Douglas, A. W.; Eskola, P.; Fisher, M. H.; Mrozik, H.; Smith, J. L.; Tolman, R. L. Avermectins. Structure Determination. *J. Am. Chem. Soc.* **1981**, *103*, 4216–4220.

Bull, D. L.; Ivie, G. W.; MacConnell, J. G.; Gruber, V. F.; Ku, C. C.; Arison, B. H.; Stevenson, J. M.; VandenHeuvel, W. J. A. Fate of avermectin B1A in soil and plants. *J. Agric. Food Chem.* **1984**, *32*, 94–102.

Davies, H. G.; Green, R. H. Avermectins and Milbemycins. *Nat. Prod. Rep.* **1986**, *3*, 87–121.

Feely, W.; Wislocki, P. G. Avermectin B_{1a} in Celery: Acetone-Unextractable Residues. *J. Agric. Food Chem.* **1991**, *39*, 963–967.

Fisher, M.; Mrozik, H. Chemistry. In *Ivermectin and Abamectin*; Campbell, W. C., Ed.; Springer-Verlag: New York, 1989; Chapter 1.

Foote, C. S. Mechanism of Addition of Singlet Oxygen to Olefins and Other Substrates. *Pure Appl. Chem.* **1971**, *27*, 635–645.

Iwata, Y.; MacConnell, J. G.; Flor, J. E.; Putter, I.; Dinoff, T. M. Residues of Avermectin B_{1a} on and in citrus fruits and foliage. *J. Agric. Food Chem.* **1985**, *33*, 467–471.

Lankas, G. R.; Gordon, L. R. Toxicology. In *Ivermectin and Abamectin*; Campbell, W. C., Ed.; Springer-Verlag: New York, 1989; Chapter 6.

Maynard, M.; Maynard, H. HPLC Assay for Avermectin B_{1a} and its Two Photoisomers using a Photo Diode Array Detector. *Bull. Environ. Contam. Toxicol.* **1989**, *43*, 499–504.

Maynard, M.; Iwata, I.; Wislocki, P. G.; Ku, C. C.; Jacob, T. A. Fate of Avermectin B_{1a} on Citrus Fruits. 1. Distribution and Magnitude of the Avermectin B_{1a} and ^{14}C Residue on Citrus Fruits from a Field Study. *J. Agric. Food Chem.* **1989a**, *37*, 178–183.

Maynard, M.; Ku, C. C.; Jacob, T. A. Fate of Avermectin B_{1a} on Citrus Fruits. 2. Distribution and Magnitude of the Aver-

mectin B_{1a} and ^{14}C Residue on Citrus Fruits from a Picked Fruit Study. *J. Agric. Food Chem.* **1989b**, *37*, 184–189.

Miwa, G. T.; Walsh, J. S.; VandenHeuvel, W. J. A.; Arison, B.; Sestokas, E.; Buhs, R.; Rosegay, A.; Avermitilis, S.; Lu, A. Y. H.; Walsh, M. A. R.; Walker, R. W.; Taub, R.; Jacob, T. A. The metabolism of avermectins B_{1a}, H_2B_{1a}, and H_2B_{1b} by liver microsomes. *Drug Metab. Dispos.* **1982**, *10*, 268–274.

Moye, H. A.; Malagodi, M. H.; Yoh, J.; Deyrup, C. L.; Chang, S. M.; Leibee, G. L.; Ku, C. C.; Wislocki, P. G. Avermectin B_{1a} Metabolism in Celery: A Residue Study. *J. Agric. Food Chem.* **1990**, *38*, 290–297.

Mrozik, H.; Eskola, P.; Reynolds, G. F.; Arison, B. H.; Smith, G. M.; Fisher, M. H. Photoisomers of Avermectins. *J. Org. Chem.* **1988**, *53*, 1820–1823.

O'Shea, K. E.; Foote, C. S. Chemistry of Singlet Oxygen. 51. Zwitterionic Intermediates from 2,4-Hexadienes. *J. Am. Chem. Soc.* **1988**, *110*, 7167–7170.

Putter, I.; MacConnell, J. G.; Preiser, F. A.; Haidri, A. A.; Ristich, S. S.; Dybas, R. A. Avermectins: Novel insecticides, acaricides, and nematicides from a soil microorganism. *Experientia* **1981**, *37*, 963–964.

Wislocki, P. G.; Grosso, L. S.; Dybas, R. A. Environmental aspects of abamectin use in crop protection. In *Ivermectin and Abamectin*; Campbell, W. C., Ed.; Springer-Verlag: New York, 1989; Chapter 13.

Received for review December 13, 1990. Accepted March 25, 1991.